SYNTHESIS OF COBALT OXIDE NANOPARTICLES FOR CATALYTIC OXIDATION OF ORGANIC POLLUTANTS

A DISSERTATION

Submitted in partial fulfillment of the

Requirements for the award of the degree

of

MASTER OF TECHNOLOGY

IN

NANOTECHNOLOGY

By

RASPAL SINGH

(17551006)

CENTER OF NANOTECHNOLOGY

INDIAN INSTITUTE OF TECHNOLOGY ROORKEE

ROORKEE-247667 (INDIA)

J2019

INDIAN INSTITUTE OF TECHNOLOGY ROORKEE

CANDIDATE'S DECLARATION

I hereby declare that the work being presented in this dissertation report entitled **"SYNTHESIS OF COBALT OXIDE NANOPARTICLES FOR CATALYTIC OXIDATION OF ORGANIC POLLUTANTS"** in partial fulfillment of the requirements for the award of the degree of **MASTER OF TECHNOLOGY** in **NANOTECHNOLOGY** submitted in the Centre of Nanotechnology, Indian Institute of Technology Roorkee, is an authentic record of my own work carried out during the period June 2018 to June 2019 under the supervision of Dr. **Vimal Chandra Srivastava**, Associate Professor, Department of Chemical Engineering, Indian Institute Of Technology Roorkee, Roorkee, India.

I have not submitted the matter embodied in this report for the award of any other degree.

Date: June 2019 **RASPAL SINGH**

Place: IIT Roorkee **Enrollment no. 17551006**

CERTIFICATE

This is to certify that the above statement made by the candidate is correct to the best of my knowledge and belief.

Dr. V. C. Srivastava
Associate Professor
Department of Chemical Engineering
Indian Institute of Technology Roorkee
Roorkee, Uttarakhand-247667

ACKNOWLEDGMENT

First and foremost, I would like to express my deep and sincere gratitude to my supervisor Dr. V. C. Srivastava, Associate Professor, Department of Chemical Engineering, Indian Institute of Technology Roorkee, for his kind cooperation and encouragement to help develop novel ideas and tackle various situations which came across while doing the project work. His constant guidance, useful criticism and constant help in the hours of need have been immensely useful. I would also like to thank and express my gratitude to Dr. R. K. Dutta, Head of the Department, Centre of Nanotechnology, Indian Institute of Technology Roorkee, for guiding and correcting various documents of mine with attention and care. I consider myself fortunate to have had the opportunity to work under their able guidance and enrich myself from their depth of knowledge.

I would like to thank Dr. Rajendra Bhatnagar, Technical superintendent, SEER Lab for his guidance in using sophisticated equipment and chemicals in the lab.

Last but not least I would also like to thank Mr. Navneet Chauhan. Mr. Ritesh Patidar, Mr. Rohit Chauhan (Ph.D. Scholars) and all my friends, colleagues and all the faculty members of Indian Institute of Technology Roorkee who in any manner directly or indirectly have put hands in any part of this dissertation work.

RASPAL SINGH
Enrollment No. 17551006
M. Tech. (Nanotechnology)
IIT Roorkee

ABSTRACT

In this study, Co_3O_4 nanoparticles were synthesized in two different solvents, one with ethanol (CoEt) and another was double-distilled water (CoDd) by precipitation-calcination method. The characterization of the prepared samples were done using X-ray diffraction (XRD), field emission scanning electron microscopy (FESEM), Brauner-Emmet-Teller (BET), thermogravimetric analysis (TGA), Fourier transform infrared spectroscopy (FTIR), dynamic light scattering (DLS) techniques. Diffraction peaks of cobalt oxalate dihydrate confirmed the synthesis of the almost pure phase of $CoC_2O_4.2H_2O$. XRD diffraction peaks of the obtained product after calcination confirms the formation of pure Co_3O_4, no other characteristic peak was obtained. TGA of CoEt and CoDd was done and phase transformation occurs at 310 ℃ and 292 ℃. However, the samples were calcined at 500 ℃ to increase crystallinity. BETshows different values of surface area for CoEt and CoDd. The surface area of CoEt was 22 m^2/g and for CoDd was 15 m^2/g. Therefore, CoEt was more porous as compared to CoDd. FTIR showed two sharp absorption peaks at 563 $cm^{-1}$and 652 cm^{-1}confirms the synthesis of Co_3O_4. Absorption peaks for CoDd observed at 540 $cm^{-1}$and 563$cm^{-1}$with slight shift. FESEM was used to determine the morphology of prepared samples. Images revealed that prepared samples were in nano range and in rod-like shapes. DLS analysis of the solution of Co_3O_4 in ethanol gives an idea about the hydrodynamic diameter of particles which was 3.96 nm for CoEt with a polydispersity index (PDI) of 0.406 while the hydrodynamic diameter of particles of CoDd was 4.131 nm with PDI of 0.413. Furthermore, we studied the effect of time on the degradation of organic compounds such as ofloxacin and pyridine with the use of Co_3O_4 nanorods complemented by H_2O_2 in a catalytic peroxidation process.

TABLE OF CONTENTS

LIST OF TABLES

LIST OF FIGURES

CHAPTER 1
INTRODUCTION

1.1. GENERAL

Safe drinkable water is a basic need for mankind in the 21thcentury. The major part of the earth's surface is water more than 70 %, out of which only 2.5% is drinkable. Most of the part (97.5 %) of surface water is sea water(salted water). Water has become polluted at a very high rate due to the mixing of untreated waste into natural water bodies. Due to the negligence of human being water contamination is becoming a real threat to the survival of the whole world. In the current age, most of the sources of water are deteriorating at a very fast rate due to industrialization. Water sources including both surface water and groundwater are contaminated due to effluents discharged from factories, water treatment plants, fertilizers, pesticides, etc.

To address the problem of water contamination several international organizations are working for this noble cause. For primary health issues, an international conference was organized in 1978 in the Soviet Union. World water conference held in Argentina in 1977. United Nation general assembly (UNGA) declared 10-year time period from 2005 to 2015 decade of "Water for Life". World health organization (WHO) had published four reports for safe drinking water.

There is a number of diseases caused due to the consumption of polluted water. Consumption of contaminated water results in 36 million deaths every year. If the water contains nitrate beyond a certain level it will cause a blue baby syndrome in children and cancer in adults. Sulfate in excess amount in water results in dehydration of the body. Diarrhea is one of the other diseases which affects a large amount of world population including deaths. Anemia, cholera, fluorosis, hepatitis, lead poisoning are some of the other diseases due to polluted water.

1.2. PYRIDINE

Pyridine (C_5H_5N) (Figure 1) is a water-soluble aromatic compound having the same structure as benzene except for nitrogen in place of carbon. Mostly it is obtained as a byproduct from coal gasification. Pyridine is a colorless compound mainly obtained from coal tar and is also used as solvents for many compounds. There are many methods for the production of

pyridine from different compounds such as acetaldehyde, ammonia, and formaldehyde. Pyridine shows electrophilic substitution, nucleophilic substitution, and radical reactions.

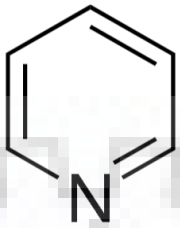

Pyridine

Fig. 1 Chemical structure of pyridine

Table 1 Chemical and physical properties of pyridine

Property Name	**Property Value**
Molecular weight	79.102 g/mol
Formal Charge	0
Color	Colorless
Odor	Nauseating
Density	0.978 g/cm^3
Boiling point	115.3 ℃
Flashpoint	20 ℃
Solubility	100 mg/mL at 21.5 ℃
Natural pH	8.5

1.3. OFLOXACIN

Ofloxacin is an antibiotic used in the medical field to treat a number of diseases such as urinary tract infection, plague, cellulitis, etc. It is also used as an eye drop and ear drop. It also leads to many side effects such as vomiting, headache, diarrhea, etc.

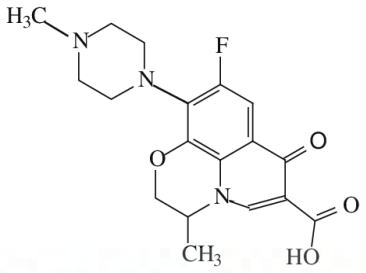

OFLOXACIN

Fig. 2 Chemical structure of Ofloxacin

Table 1 Chemical and physical properties of Ofloxacin

Properties	Property Value
Molecular Weight	361.373 g/mol
Formal Charge	0
Color	White to pale yellow
Melting point	254 ℃
Solubility	283 mg/mL in water

1.4. Co_3O_4 NANOPARTICLE

Cobalt oxide (Co_3O_4) is a very strong catalyst for reduction. Thermodynamic stability of Co_3O_4 nanoparticles so it could be used as a catalyst. It is also used for decomposition of NO_x type of compounds. SBA-15 supported cobalt oxide nanoparticles are very efficient for the decomposition of N_2O. Co_3O_4 has have been widely used in the area of magnetic materials, heterogeneous catalyst, lithium-ion batteries, dye degradation, oxidation of vehicle exhaust gas sensing materials. Pudukudy et al. [2013] prepared spinel Co_3O_4 nanoparticles by sol-gel method and applied as photocatalyst for the degradation of methylene blue dye under UV light irradiation.

Several methods have been applied for the synthesis of Co_3O_4 nanoparticles of different morphology. Such that solvothermal, hydrothermal, thermal dissociation, precipitation followed calcination and many more. Precipitation-calcination method is a very good option because it is a

simple and cheap method. Sun et al. [2016] used this method for the synthesis of porous α-$F_e2O_3$nanorods. It is a two-step method, in first of precipitation step metal oxalate formed. This metal oxalate works as a sacrificial template and in the second step of calcination and hence metal oxide formed.

Various coating techniques had been used for producing thin films of Co_3O_4 nanoparticles. Pulsed laser deposition (PLD), spin coating, dip coating, electron beam deposition, and sol-gel deposition are the most used techniques. Edla et al. [2014] prepared coating of Co_3O_4 nanoparticles by a pulsed laser deposition method. Melzer et al. [2017] used chemical vapor deposition at low temperature to prepare anode of Co_3O_4 nanoparticles for lithium-ion batteries. Raja et al. [2007] used dip coating for coating of cobalt oxide nanoparticles upon PTFE substrate.

We adopted the process of catalytic peroxidation (Yadav and Srivastava, 2017) for the degradation of ofloxacin and pyridine. This method utilizes the ability of a catalyst to enhance the mineralization activity of hydrogen peroxide by increasing the generation of hydroxyl radical ions. These radical ions can oxidize with the obnoxious organic compounds and oxidize them to simpler compounds.

CHAPTER 2
LITERATURE REVIEW

Warning et al. [2012] prepared the coating of Co_3O_4 nanoparticles by various methods i.e. pulsed laser deposition, electron beam deposition and sol-gel method and electro less deposition techniques. Prepared coatings were characterized by SEM, TEM, XRD, XPS, and UV–vis spectroscopy. Cobalt chloride and diluted ammonia solution were used as starting materials. These coatings were applied for the degradation of methylene blue dye. Manigandan[a] et al. [2013]prepared cobalt oxide nanoparticles by thermal decomposition of $Co(OH)_2$. $Co(OH)_2$ was prepared from cobalt oxide, NH_4OH and glycerol. $Co(OH)_2$ was calcined at 450 °C. the prepared sample was characterized by XRD, FTIR and SEM. XRD confirms good crystallinity and phase. Presence of functional group was done with the help of FTIR. Nano dimension was done with SEM. Cobalt oxide nanoparticles was applied for detection of nitrobenzene. Cobalt chloride was used as precursor along with ammonium hydroxide (NH_4OH), potassium hydroxide (KOH). Lagerqvist et al. [2014]used spin coating for a thin film of cobalt oxide and composites and then heating at 500 °C in a different atmosphere. Cobalt nitrate and cobalt acetate were used as precursor and methanol as solvent. Spin coating was done at three different speed (1000, 2000, 3000). Morphology of the prepared sample film was done by XRD. Calcination temperature was decided by the TGA curve.

Mahajan et al. [2019]. Pyridine and quinoline were degraded in this study. Both of these compounds are heterocyclic. For completion of reaction, photo-catalysts were used. The photo-catalysts used is Cu doped ZnO. This photo-catalyst has been synthesized with different amount of doping of Cu. The different amounts of doping synthesized are 1%, 5%, 10%. The method used for photo-catalyst synthesis is precipitation method. Field emission scanning electron microscopy (FE-SEM), transmission electron microscopy (TEM), X-ray diffraction (XRD), Brunauer Emmett Teller (BET), diffuse reflectance spectroscopy (DRS) and photoluminescence (PL) techniques are used for the purpose of the characterization of catalysts. Authors used different doping of Cu in ZnO. The band gap of ZnO with 1% of Cu doping was found to be 3.21 eV. The band gap of ZnO with 5% of Cu doping was found to be 3.17 eV. The band gap of ZnO with 10% of Cu doping was found to be 2.91 eV. The band gap found for pure ZnO is 3.27 eV. The variables studied are pH, photo-catalyst dose and time irradiation. Under optimum

conditions (5% Cu doped ZnO, a dose of 1.2 g L^{-1} for pyridine and 1.6 g L^{-1} for quinoline, pH = 11 and time = 5 h), the maximum pyridine and quinoline mineralization efficiencies were found to be 92.4% and 74.3%, respectively. Mineralization of pyridine was studied as first-order kinetics. Reactive oxygen species (ROS) scavenger studies has to be used for the conformation of the generation of singlet oxygen, hydroxyl radicals and superoxide radicals. It was found that the excellent mineralization process took place during this study. This has been established by catalyst reusability. The mineralization took place till four consecutive cycles. The band structures were compared with respect to the potential of highly reactive species (•OH and $O_2^{\bullet-}$). By this comparison, the enhanced photo-catalytic mechanism was examined. There may be various methods of proposing pathways of mineralization. In this study, the method of finding out the pathway of mineralization on the basis of the intermediates detected by gas chromatography coupled with mass spectrometry (GC-MS) analysis.

Subbaramaiah et al. [2013] used Cu-loaded Santa Barbara amorphous (SBA-15) catalysts were generated in this study. The method used for this synthesis is the impregnation method. This is later utilized for catalytic wet peroxide oxidation (CWPO) of pyridine from aqueous solution. In this synthesis, hydrogen peroxide is used as the oxidant. Brunauer–Emmett–Teller (BET) surface area: temperature-programmed reduction, H_2-chemisorption, Fourier transform infrared spectroscopy, and field emission scanning electron microscopy are used for the characterization of synthesized catalysts. Results obtained by characterization shows that the Cu species are distributed inside the porous structure of SBA-15. The effect of various parameters such as Cu loading on SBA-15, pH, catalyst dose, H_2O_2 concentration, and temperature have been studied for their effect on CWPO of pyridine. More than 97% pyridine removal and 92% total organic carbon removal was achieved at optimum condition. Cu/SBA-15 showed stable performance during reuse for six cycles with negligible copper leaching.

Jin et al. [2018] successfully synthesized rod-like nanoparticles of cobalt oxide using ethanol as solvent. Cobalt nitrate is used as a precursor with oxalic acid and after mixing, oxalate precursor is formed. The obtained powder was calcinated at 500 ℃ instead of 300 ℃ for better crystallinity. Prepared oxide powder was characterized by TEM, FESEM, XRD, TGA, BET, and DTA. XRD analysis confirms pure phase and FESEM confirm nano dimension of powder oxide. The surface area of the sample was 28.42 m^2/g. Abdelhak et al. [2018] prepared a manganese-doped cobalt oxide nanoparticles coating. Method of the coating was dip coating along with the

sol-gel method. Manganese used from 0 % to 9 % in concentration. The prepared coating was characterized by UV-visible spectroscopy, XRD and FTIR. Cobalt nitrate hexahydrate ($Co(NO_3)_2.6H_2O$) used as precursor along with sucrose ($C_{12}H_{22}O_{11}$).

Amri et al. [2012] used a dip coating technique for preparation of coating of copper-cobalt oxide on the substrate of aluminum. Phase structure was characterized by X-ray Diffraction (XRD). FESEM confirms that prepared samples are of nano dimensions. To investigate the reflectance of prepared coating UV-Vis-NIR spectrophotometry was used. Nanoparticles were formed by sol-gel method. Abdelhak et al. [2019] used sol-gel method followed by a dip coating method for coating of manganese doped cobalt oxide nanoparticles. Glass was used as a substrate. Prepared coatings were characterized by UV-Vis spectroscopy, XRD, FTIR, and complex impedance spectroscopy. doping of Mn varies from 0 % to 9 %. For the different concentration of Mn, different values of energy bandgap (E_g) were obtained. Upasen etc. [2017] used thermal decomposition to prepare nanoparticles of cobalt oxide. Cobalt acetate was used as a precursor, oleic acid as a capping agent and for reduction, $NaBH_4$ was used. There were three types of solvent (hexane, xylene and acetone) were used. To study the effect of various solvents upon the properties of cobalt oxide were investigated by XRD, TGA, TEM, and FTIR. The same crystal structure was observed for all three samples. Particle size and specific surface area were different for all three samples.

CHAPTER 3
OBJECTIVES

The main objective of this present work was to synthesize cobalt oxide nanoparticles and use them for catalytic oxidation of organic pollutants such as pyridine and ofloxacin. Based on the literature review, the following objectives were set for the present study:

- To prepare cobalt oxide (Co_3O_4) nanoparticles in different solvents by precipitation followed by calcination method.
- To analyze the properties of prepared cobalt oxide nanoparticles by various characterization techniques such as X-ray diffraction (XRD), field emission scanning electron microscope (FESEM), thermogravimetric analysis (TGA), differential thermal analysis (DTA), Fourier transform infrared spectroscopy (FTIR), Brunauer-Emmet-Teller (BET), and dynamic light scattering (DLS).
- To use the prepared nanoparticles for catalytic oxidation of organic pollutants such as pyridine and ofloxacin.
- To study the degradation of the organic pollutant with respect to the time.

CHAPTER 4
EXPERIMENTAL

Experiments were conducted in a 250 mL three-neck flask with a flat bottom fitted with an oil bath to maintain the temperature. This system was set up in a reflux manner to avoid any loss of vapors to the atmosphere. For each run, a 100 mL sample of ofloxacin/pyridine solution (100 ppm) was taken and heated to a temperature of 55 ℃, followed by the addition of hydrogen peroxide (2 µL) and Co_3O_4 nano-rods (100 mg). The degradation of ofloxacin and pyridine in the presence of catalyst without the addition of hydrogen peroxide was ~5% and ~3%, respectively. Samples were taken after every one hour during the degradation process in an aliquot (1.5 mL) and were analyzed by UV spectroscopy. The concentrations were calculated based on the respective calibration curves prepared beforehand.

4.1. MATERIALS

Cobalt (II) chloride hexahydrate ($CoCl_2.6H_2O$, A.R. grade, 99.0% pure), oxalic acid dihydrate ($C_2H_2O_4.2H_2O$, A.R. grade, 99.5% pure) were purchased from SRL Limited. absolute ethanol (C_2H_5OH, L.R. grade, 99.9% pure) was purchased from Changshu Hongsheng Fine Chemical Co. Ltd. Double distilled water was used throughout. All the chemicals were used without any further purification.

4.2. CATALYST PREPARATION

Co_3O_4 nanorods (CoEt) were synthesized by precipitation followed by calcination method. In the synthesis process of catalyst 0.237 g of $CoCl_2.6H_2O$ was added into 25mL of absolute ethanol in magnetic stirrer for 30 minutes up to complete dissolution. 1.26 g oxalic acid was dissolved in 10 mL absolute ethanol using magnetic stirrer. After that solution of oxalic acid was added drop by drop into cobalt solution under magnetic stirring. The solution was allowed to stir for 30 minutes after that precipitate was collected and centrifuged with double distilled water for six times and dried in an oven at 80 ℃ for 10 hours to obtain oxalate precursor. Now obtained oxalate precursor was calcined in a muffle furnace at 500 ℃ for 2 hours. A second catalyst (CoDd) was also prepared by taking double distilled water as solvent by the same method.

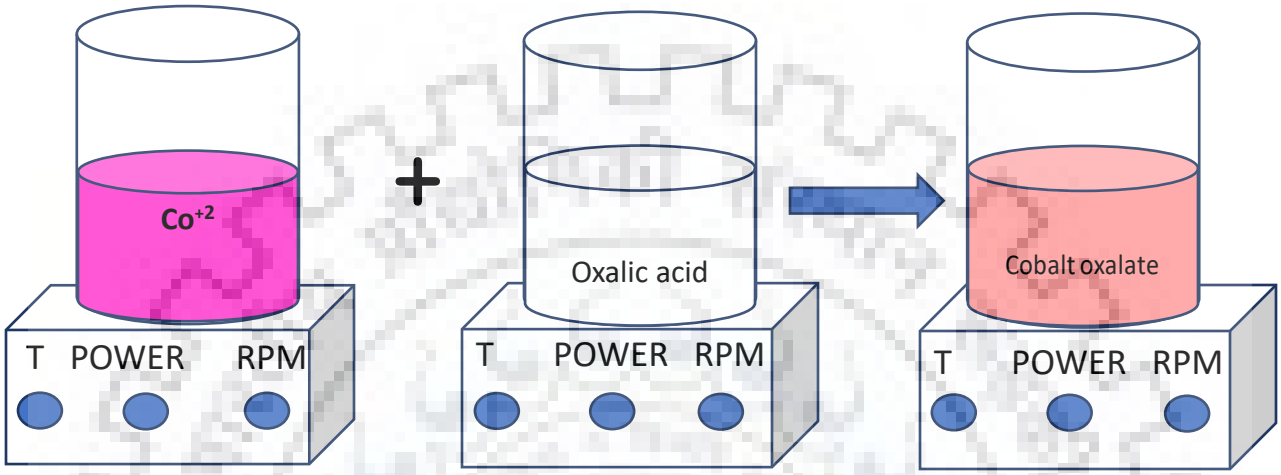

Fig . 3 Synthesis of cobalt oxalate precursor

4.3. OVERVIEW OF CATALYST CHARACTERIZATION TECHNIQUES

4.3.1. X-ray diffraction (XRD)

For analysis of phase structure, purity and crystalline nature of as-synthesized nanorods XRD technique are used which is a fingerprinting tool for that. XRD technique is widely used for quantitative and qualitative phase analysis throughout industry and research institutes. In our case, we used a Bruker D8 advance model of a wide-angle range of 5º to 120º on a scale range of 2θ with a scanning rate of 4º/min.

4.3.2. Field emission scanning electron microscopy (FE-SEM)

FE-SEM is used for the image of morphology of catalyst at the microscopic level. It is widely used in the field of bioscience, chemistry, and physics for research purpose. It can observe to nanoscale level at the surface of materials and cells. FESEM scan the object with the help of generated electron by field emission source. These generated electrons (primary electrons) are accelerated in high electric field gradient are diverted by electronic lenses to produce a narrow beam of electrons. This narrow beam bombards at an object and produces secondary electrons from the object. Detector catches velocity and angle of secondary electrons and convert into an electronic signal, which is further amplified and transformed into an image.

4.3.3. Thermogravimetric analysis (TGA)

In this technique, a given sample is heated in a controlled atmosphere. The objective of TGA is to measure the change in weight of sample with temperature and time. After knowing the initial weight of the sample, the temperature is increased at a constant level and the corresponding change in weight is recorded. After that, a plot is drawn between percentage weight change and temperature which is known as the thermogravimetric curve.

4.3.4. Differential thermal analysis (DTA)

In this technique, a sample and a reference material both heated at the same rate in an oven and temperature difference between sample and reference material are recorded. If during the heating sample absorbs or evolve enthalpy of transition, then its temperature differs from reference material and this difference is recorded. If the sample undergoes the endothermic process, the temperature of the sample will be less than reference. On the other hand, the temperature of the sample will be greater than reference in case of exothermic process.

4.3.5. Brunauer-Emmet-Teller (BET)

This technique is useful in calculating of surface area, pore size, and pore volume. Pore are formed generally calcination of precipitates. Dinitrogen (N_2) gas is used mostly for calculating surface area. Surface area is determined by adsorption followed condensation of N_2 gas at 77 K. firstly vacuum is created in the chamber and then cooling to 77 K by liquid N_2. After that partial pressure of N_2 gas is increased due to which some amount of gas is adsorbed by the sample. After some time, equilibrium is reached and corresponding pressure is recorded. This procedure is repeated and a plot is drawn between relative pressure (p/p_o) and the amount of gas adsorbed by the sample.

4.3.6. Fourier-transform infrared spectroscopy (FTIR)

This technique is useful to identify types of bonds in molecular species, mainly organic compounds. When infrared radiation passes through the sample, some part of this radiation was absorbed by sample and rest transmitted. A spectrum is created by absorption and transmission frequency. Since every bond or functional group have unique absorption frequency so also spectrum will be unique for every bond or functional group.

4.3.7. Dynamic light scattering (DLS)

Hydrodynamic diameter and size distribution of particles in the suspension can be determined by dynamic light scattering. Scattering happens when light colloid with particles. DLS is applied for the determination of the size of particles like proteins, polymers, nanoparticles, bio cells.

CHAPTER 5
RESULTS AND DISCUSSION

After the synthesis of catalyst next step is characterization. The phase structure and its purity of the catalyst are investigated by XRD (Bruker/D8 model). Thermal analysis of the oxalate precursor was carried out on an (S11 6300 EXSTAR) thermal analyzer in air atmosphere. Morphology of the sample was investigated by FESEM (Carl Zeiss (Zamini-300)). TEM (FEI Tecnai G^2 20 S-Twin) was used for microstructure analysis. The surface area of the Co_3O_4 powder was calculated by Brunauer-Emmett-Teller (BET). Chemical analysis of the sample was done with the help of FTIR. The absorbance of the sample done with UV-vis-spectrophotometer. The hydrodynamic size was calculated by Dynamic Light Scattering (DLS).

The total mineralization for pyridine can be represented as:

$$\mathbf{C_5H_5N + 14.5\ H_2O_2 \rightarrow 5\ CO_2 + 17\ H_2O + NO_2} \quad \text{(i)}$$

For the complete mineralization of pyridine, we calculated the amount of 30% H_2O_2 solution which will be required. For one mole of pyridine, we require 493.14 g of H_2O_2. This means that 1643.8 g of H_2O_2 will be required. Thus the volume of H_2O_2 solution required for the complete mineralization is calculated to be 1.8 mL for 1 L of 100 mg pyridine solution.

5.1. CATALYST CHARACTERISATION

5.1.1. Thermal analysis

Thermal analysis experiment of the prepared CoEt of oxalate precursor $CoC_2O_4.2H_2O$ (Fig. 4) is performed (air atmosphere) to take a look into the phase transformation with temperature change. This experiment is performed between a temperature range of 30 ℃ to 700 ºC. First weight loss is observed between 134-208 ℃ in the TG curve, which is attributed to the conversion of $CoC_2O_4.2H_2O$ to CoC_2O_4. In DTA curve this can confirm by an endothermic peak. Weight loss in the first process is 19.02 %. Second phase transformation process observed from 283-310 ºC, which corresponds to a strong exothermic peak in the DTA curve. This can be attributed to the transformation of $CoC_2O_4$to Co_3O_4. In second phase36.78 % weight loss is seen.

Thermal analysis for CoDd (Fig. 5) reveals that the first transformation process occurs between 137-201 ℃ corresponding a small endothermic peak in the DTA curve. The second phase occurs from 269-300 ℃ corresponding a strong peak in the DTA curve.

The samples of oxalate precursors were calcined at 500 ℃ to obtain good crystallinity of final powder (Co_3O_4).

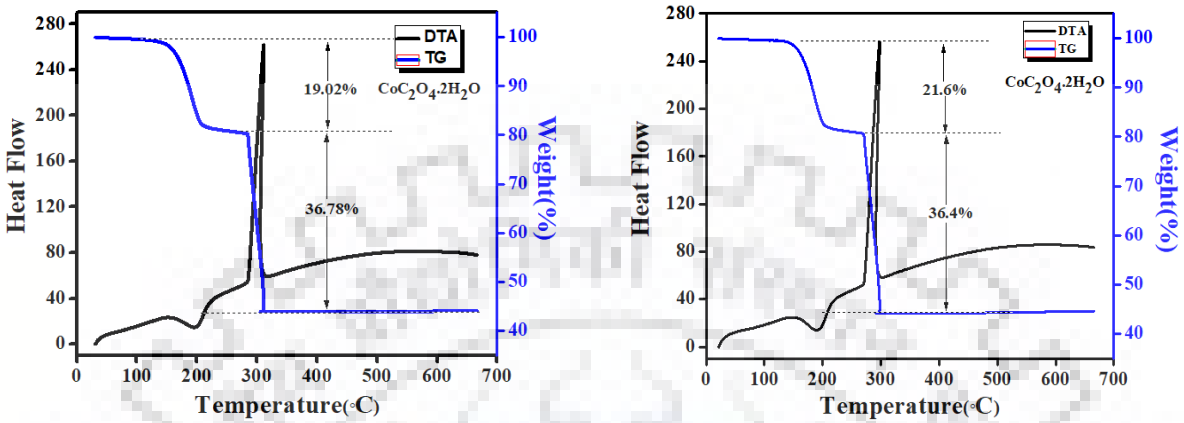

Fig. 4 & Fig. 5 TG and DTA curve of cobalt oxalate

5.1.2 Structural analysis

The phase structure and purity of oxalate precursor ($CoC_2O_4.2H_2O$) (Fig. 6) and cobalt oxide (Co_3O_4) were investigated by XRD pattern of samples. Diffraction peaks of oxalate precursor obtained from CoEt confirm the synthesis of the almost pure phase of $CoC_2O_4.2H_2O$. XRD diffraction patterns of the obtained product after calcination at 500 ºC, confirms the formation of pure Co_3O_4phase. All the diffraction peaks can be indexed to the cubic structure of Co_3O_4, no other characteristic peak is obtained hence no impurity is present in the final sample after calcination.

Phase structure and purity of prepared oxalate precursor and cobalt oxide were investigated by XRD diffraction peaks. Fig. 7 confirms the formation of the almost pure phase of $CoC_2O_4.2H_2O$ and Fig. 3d confirms the formation of pure Co_3O_4. Final product Co_3O_4 is pure because no characteristic peak of any impurity is obtained.

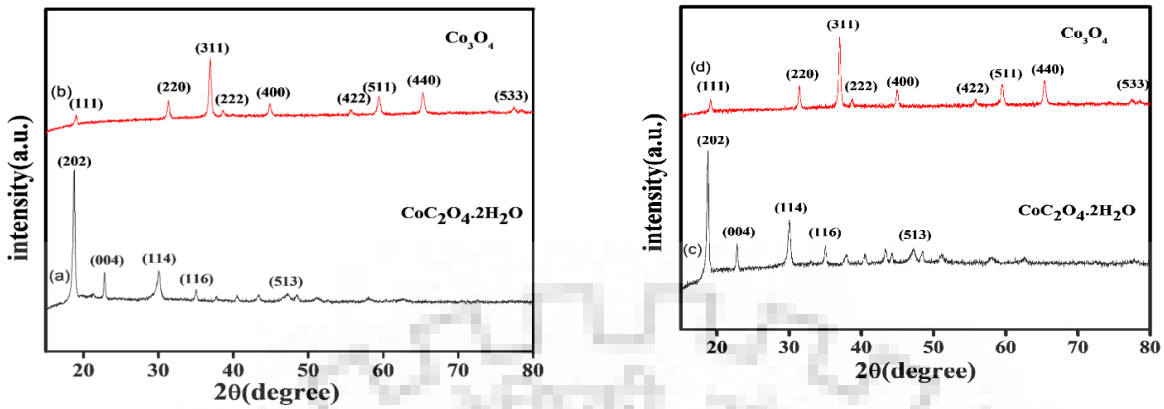

Fig. 6 & Fig. 7 XRD patterns of (c) CoC_2O_4 and (d) Co_3O_4

5.1.3. Textural analysis

The surface area of the prepared CoEt was investigated by BET surface area analyzer. The sample was dried in an oven overnight to remove moisture content and then a measured quantity of sample was degassed by nitrogen gas at 150 ℃ for 5 hours. After degassing remaining sample was put under the testing machine for 7 hours. Analysis of data obtained from bet analyzer revealed that the surface area of CoEt (Fig 8) was 22.0348 m^2/g.

The surface area of the prepared CoDd was investigated by BET surface area analyzer. The sample was dried in an oven overnight to remove moisture content and then a measured quantity of sample was degassed by nitrogen gas at 150 ℃ for 5 hours. After degassing remaining sample was put under the testing machine for 7 hours. Analysis of data obtained from bet analyzer revealed that the surface area of CoDd (Fig 9) was 15.7176 m^2/g.

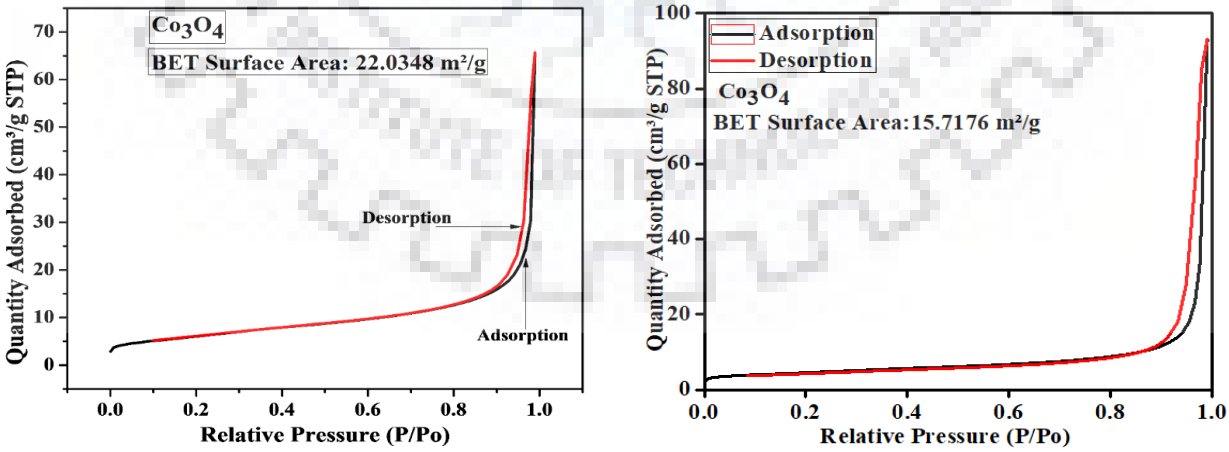

Fig. 8 & Fig. 9 N_2 adsorption-desorption isotherm of the Co_3O_4 nanoparticle

5.1.4. Morphology

Morphology of the Co_3O_4 powder (CoEt) was investigated by nondestructive technique FESEM by Carl Zeiss Ultra Plus FE-SEM. FE-SEM use electrons for sample imaging. Results are shown in Fig. 10 at three different scales 100 nm, 200 nm, and 1 μm and 2 μm. From Fig. 10. it is clear that prepared powder is in the form of nanorods.

Morphology of the Co_3O_4 powder (CoDd) was investigated by FESEM technique by Carl Zeiss Ultra Plus FESEM. FESEM use electrons for sample imaging. Results are shown in Fig.11 at three different scales 100 nm, 200 nm, and 1 μm and 2 μm. From Fig. 11. it is clear that prepared powder is in the form of nanorods.

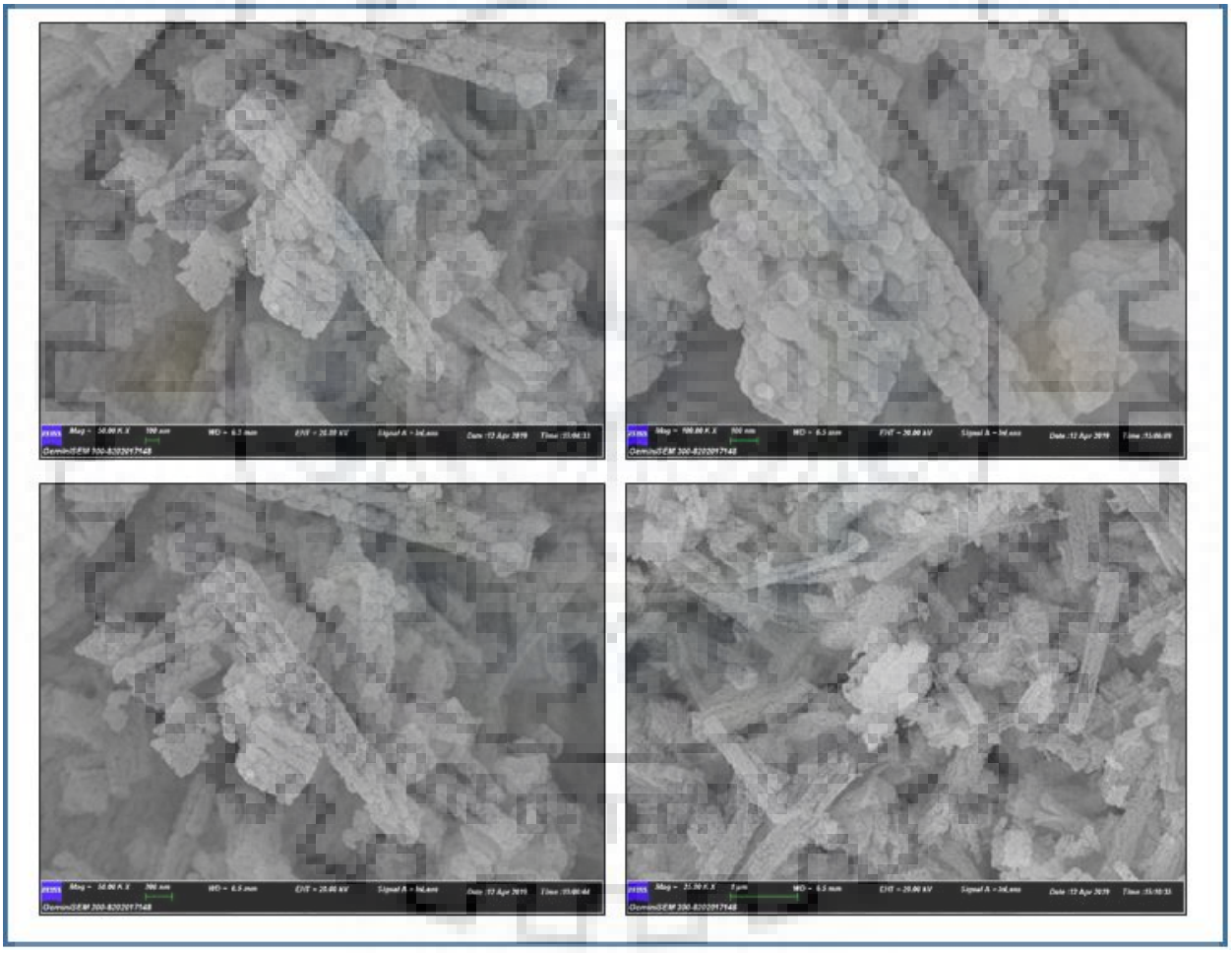

Fig. 10 FESEM images of prepared Co_3O_4 nanoparticles (solvent-ethanol) at a different scale

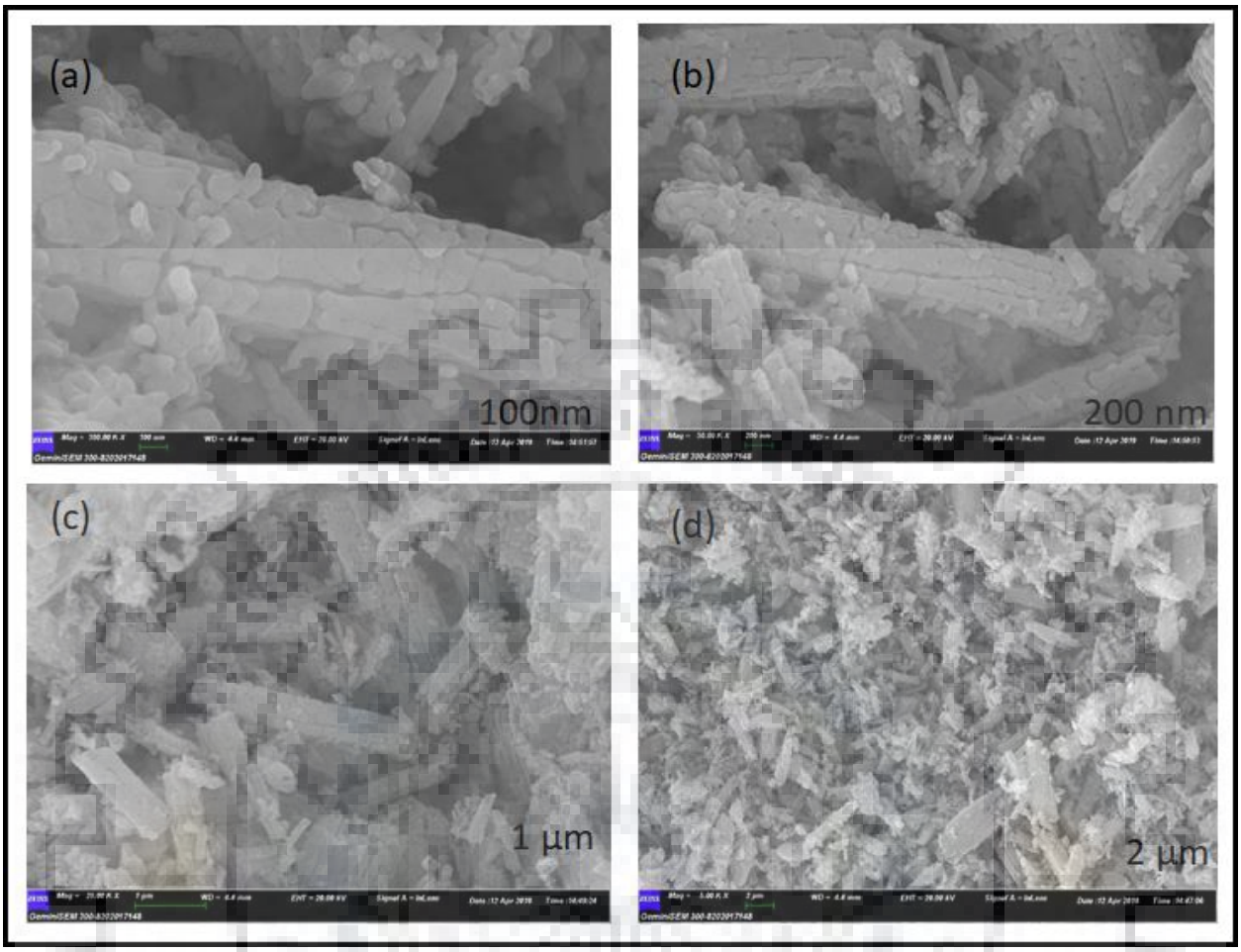

Fig. 11 FE-SEM images of prepared Co_3O_4 nanoparticles (solvent-ethanol) at a different scale

5.1.5. FTIR analysis

FTIR analysis was done by Cary 630 FTIR Spectrometer. Fig. 12 shows an IR spectrum of CoEt respectively. FTIR spectrum of CoEt shows two different absorption peaks at 563 (ν_1) and 652 (ν_2) cm^{-1} which generates due to stretching vibration of metal-oxygen bond and confirm the synthesis of cobalt oxide. The (ν_1) band is attributed to vibration of the Co^{3+}in the octahedral hole. (ν_2) the band is characteristics of Co^{2+}vibration in a tetrahedral hole in the lattice.

FTIR analysis was done by Cary 630 FTIR Spectrometer. Fig. 13 shows an IR spectrum of CoDd, respectively. FTIR spectrum of CoEt shows two different absorption peaks at 540 (ν_1) and 652 (ν_2) cm^{-1} which generates due to stretching vibration of metal-oxygen bond and confirm the synthesis of cobalt oxide. The (ν_1) band is attributed to vibration of the Co^{3+}in the octahedral hole. (ν_2) the band is characteristics of Co^{2+}vibration in a tetrahedral hole in the lattice.

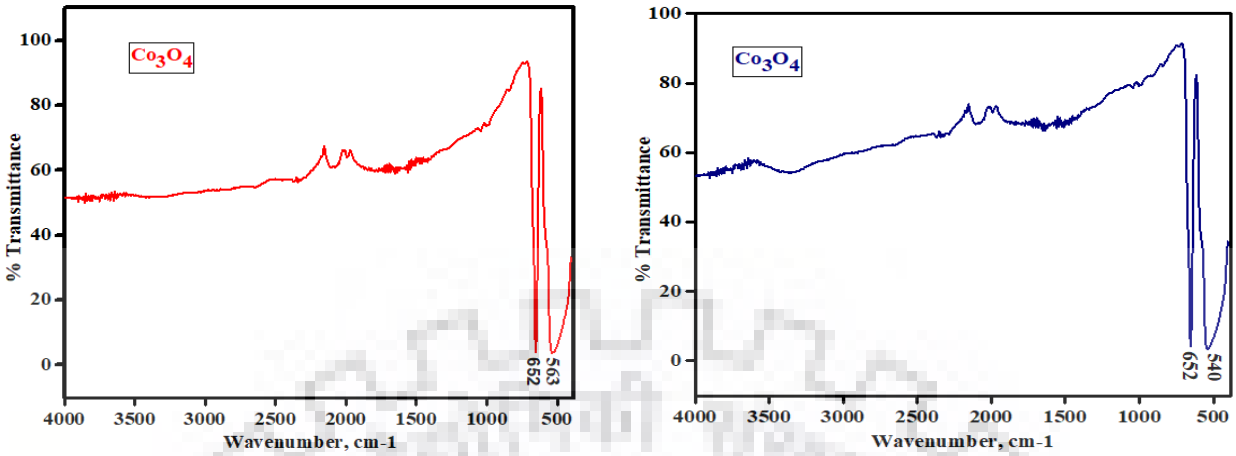

Fig. 12 & Fig. 13 FTIR spectrum of Co_3O_4 nanoparticle

5.1.6. Dynamic light scattering (DLS)

The average hydrodynamic diameter of prepared CoEt and CoDd was determined by Zetasizer nano zs. Fig. 14 and 15 showsAverage nanoparticle size was 3.96 nm with a polydispersity index (PDI) of 0.406 for CoEt. Average nanoparticle size was 4.131 nm with a polydispersity index (PDI) of 0.413 for CoDd. Average hydrodynamic size confirms the synthesis of a particle in nano range.

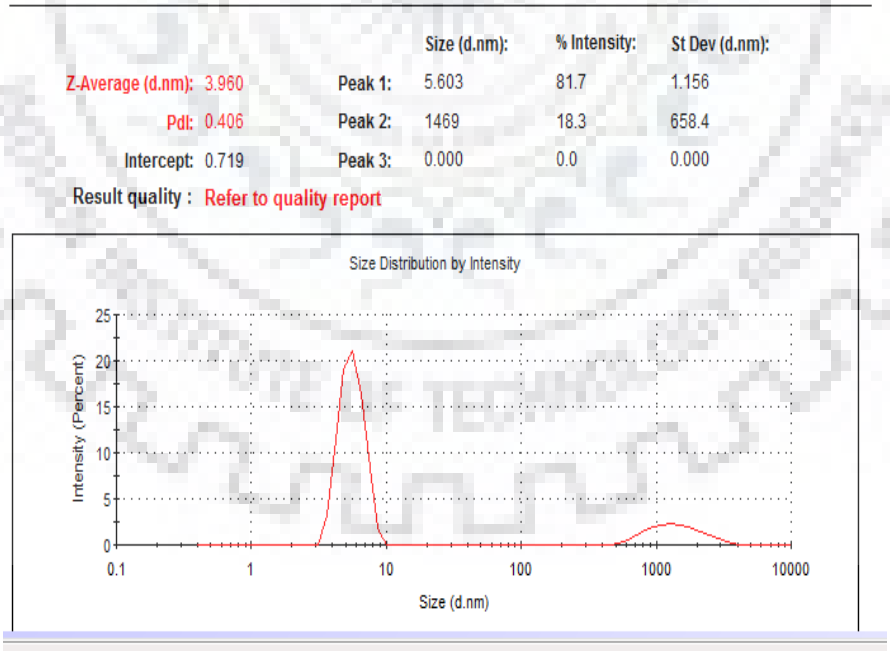

Fig. 14 DLS spectrum of showing size distribution by volume

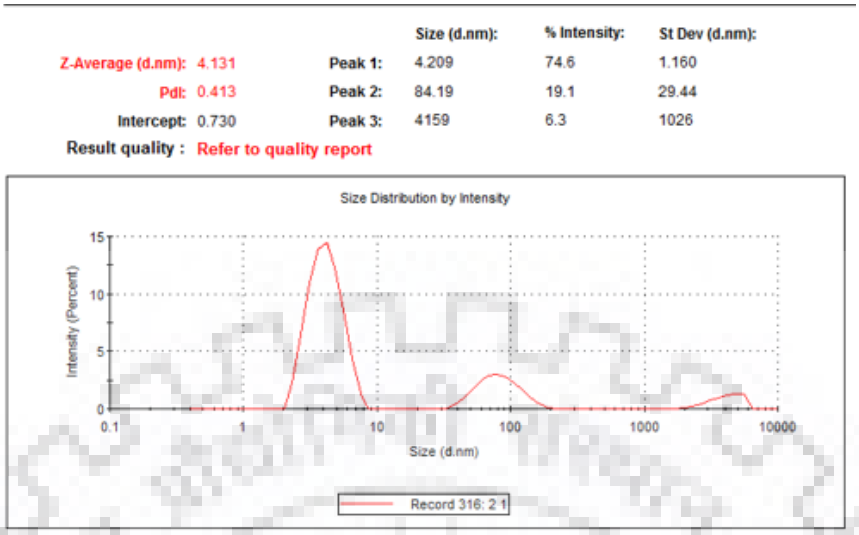

Fig. 15 DLS spectrum of showing size distribution by volume

5.2. CATALYST PEROXIDATION STUDIES FOR OFLOXACIN AND PYRIDINE

The effect of time was studied on the peroxidation process using the as-synthesized nano-rods. The results are shown in Fig. 16 and Fig. 17. In the case of mineralization of pyridine with Co_3O_4 nanorods and H_2O_2, the percentage of degradation was 53% in a total of 5 hours, while in the case of ofloxacin it was 64% in 5 hours. This shows that pyridine is a difficult heterocyclic nitrogenous compound to breakdown rather than ofloxacin, despite a lower molecular weight. This could be attributed to the fact that pyridine has an N atom present within the aromatic ring.

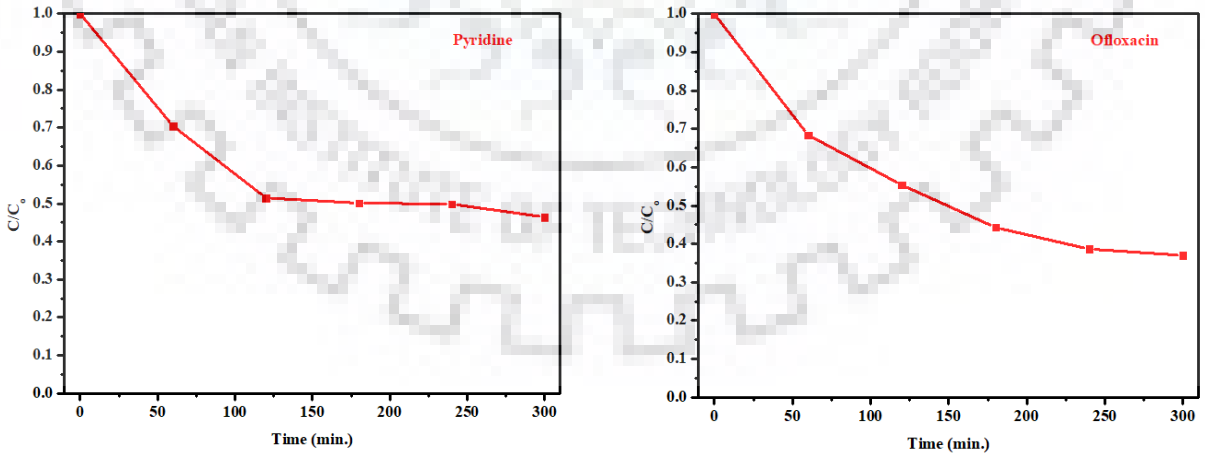

Fig. 16 & Fig. 17 Change in the concentration of ofloxacin during peroxidation with Co_3O_4 nano-rods

CHAPTER 6

CONCLUSION AND RECOMMENDATION

6.1. CONCLUSION

The objective of this work was to prepare nanoparticles in two different solutions (absolute ethanol and double distilled water). Properties of prepared samples were investigated by different techniques. Following conclusions can be drawn from this work:

- X-ray diffraction (XRD) analysis showed that the prepared final product is crystalline in nature. Diffraction peaks of cobalt oxalate dihydrate confirmed the synthesis of the almost pure phase of $CoC_2O_4.2H_2O$. XRD diffraction peaks of the obtained product after calcination confirms the formation of pure Co_3O_4, no other characteristic peak was obtained.
- Brunauer-Emmet-Teller (BET) shows different values of surface area for CoEt and CoDd. The surface area of CoEt was 22.0348 m^2/g and for CoDd was 15.7176 m^2/g. Therefore, CoEt was more porous as compared to CoDd.
- Field emission scanning electron microscopy (FESEM) was used to determine the morphology of prepared samples. Images revealed that prepared samples were in nano range and in rod-like shapes.
- Thermo-gravimetric analysis (TGA) of the samples showed us that phase transformation temperature for CoEt was 292 ℃ and for CoDd was 310 ℃. same can be confirmed from differential thermal analysis (DTA) curve.
- Fourier transform infrared (FTIR) showed two sharp absorption peaks at 563 $cm^{-1}$and 652 cm^{-1}confirms the synthesis of Co_3O_4. Absorption peaks for CoDd observed at 540 $cm^{-1}$and 563$cm^{-1}$with slight shift.
- Dynamic light scattering (DLS) analysis of the solution of Co_3O_4 in ethanol gives an idea about the hydrodynamic diameter of particles. Size of particles of CoEt was 3.96 nm with a polydispersity index (PDI) of 0.406. size of CoDd was 4.131 nm with a polydispersity index (PDI) of 0.413.
- In the case of catalytic peroxidation of pyridine with Co_3O_4 nanorod activated H_2O_2, the percentage of mineralization is 53% in 5 hours, while in the case of ofloxacin it is

64% in 5 hours. This shows the potential use of Co-based nano-morphologies in the activation of hydrogen peroxide-based peroxidation of heterocyclic compounds.

6.2. RECOMMENDATIONS

Following recommendations are suggested for further studies:

- To achieve higher removal percentage of ofloxacin and pyridine by using UV light.
- The same catalyst can be used in sunlight.
- Compare the removal efficiency of ofloxacin and pyridine using both samples.

REFERENCES

Angeles-Hernández, Mauricio J., Gary A. Leeke, and Regina CD Santos. "Catalytic supercritical water oxidation for the destruction of quinoline over MnO_2/CuO mixed catalyst." Industrial & Engineering Chemistry Research 48.3 (2008): 1208-1214.

B. Yadav and V. C. Srivastava, Catalytic peroxidation of recalcitrant quinoline by ceria impregnated granular activated carbon, Clean Technol. Environ. Policy, (2017): 1547 -1555.

Choi, Kwon-Il, Hae-Ryong Kim, Kang-Min Kim, Dawei Liu, Guozhong Cao, and Jong-Heun Lee. "C_2H_5OH sensing characteristics of various Co_3O_4 nanostructures prepared by solvothermal reaction." Sensors and Actuators B: Chemical146, no. 1 (2010): 183-189.

Daly, Brian, Donna C. Arnold, Jaideep S. Kulkarni, Olga Kazakova, Matthew T. Shaw, Sergey Nikitenko, Donats Erts, Michael A. Morris, and Justin D. Holmes. "Synthesis and characterization of highly ordered cobalt–magnetite nanocable arrays." Small 2, no. 11 (2006): 1299-1307.

D. Rajamanickam and M. Shanthi , Photocatalytic degradation of an organic pollutant by zinc oxide – solar process, Arabian J. Chem., (2016): S1858 -S1868.

D. Rameshraja , V. C. Srivastava , J. P. Kushwaha and I. D. Mall , Competitive adsorption isotherm modelling of heterocyclic nitrogenous compounds, pyridine, and quinoline, onto granular activated carbon and bagasse fly ash, Chem. Pap., (2018): 617 -628.

Garg, Shweta, Vimal Chandra Srivastava, Seema Singh, and Tapas Kumar Mandal. "Catalytic degradation of pyrrole in aqueous solution by Cu/SBA-15." International Journal of Chemical Reactor Engineering 13, no. 3 (2015): 437-445.

Gong, Yuxiao, Yan Wang, Guang Sun, Tiekun Jia, Lei Jia, Fengmei Zhang, Long Lin, Baoqing Zhang, Jianliang Cao, and Zhanying Zhang. "Carbon nitride decorated ball-flower like Co_3O_4 hybrid composite: Hydrothermal synthesis and ethanol gas sensing application." Nanomaterials 8, no. 3 (2018): 132.

Guimaraes, Iara R., Amanda Giroto, Luiz CA Oliveira, Mario C. Guerreiro, Diana Q. Lima, and José D. Fabris. "Synthesis and thermal treatment of Cu-doped goethite: oxidation of quinoline through heterogeneous Fenton process." Applied Catalysis B: Environmental 91, no. 3-4 (2009): 581-586.

Hu, Linhua, Qing Peng, and Yadong Li. "Selective synthesis of Co_3O_4 nanocrystal with different shape and crystal plane effect on catalytic property for methane combustion." Journal of the American Chemical Society 130, no. 48 (2008): 16136-16137.

Kim, Youngjun, Jung-Hyun Lee, Sungeun Cho, Yongwoo Kwon, Insik In, Jihoon Lee, Nam-Ho You et al. "Additive-free hollow-structured Co_3O_4 nanoparticle Li-ion battery: the origins of irreversible capacity loss." ACS nano 8, no. 7 (2014): 6701-6712.

Koo, Won-Tae, Sunmoon Yu, Seon-Jin Choi, Ji-Soo Jang, Jun Young Cheong, and Il-Doo Kim. "Nanoscale PdO catalyst functionalized Co_3O_4 hollow nanocages using MOF templates for selective detection of acetone molecules in exhaled breath." ACS applied materials & interfaces 9, no. 9 (2017): 8201-8210.

K. V. Padoley , S. N. Mudliar and R. A. Pandey , Heterocyclic nitrogenous pollutants in the environment and their treatment options – An overview, Bioresour. Technol., (2008): 4029 - 4043.

Li, Yanwei, Na Luo, Guang Sun, Bo Zhang, Guangzhou Ma, Honghong Jin, Yan Wang, Jianliang Cao, and Zhanying Zhang. "Facile synthesis of $ZnFe_2O_4$/α-Fe_2O_3 porous microrods with enhanced TEA-sensing performance." Journal of Alloys and Compounds 737 (2018): 255-262.

Lü, Yinyun, Wenwen Zhan, Yue He, Yiting Wang, Xiangjian Kong, Qin Kuang, Zhaoxiong Xie, and Lansun Zheng. "MOF-templated synthesis of porous Co_3O_4 concave nanocubes with high specific surface area and their gas sensing properties." ACS applied materials & interfaces 6, no. 6 (2014): 4186-4195.

Mahajan, Bharat Kumar, Navneet Kumar, Rohit Chauhan, Vimal Chandra Srivastava, and Siddhant Gulati. "Mechanistic evaluation of heterocyclic aromatic compounds mineralization by a Cu doped ZnO photo-catalyst." Photochemical & Photobiological Sciences (2019): 883 -889.

Nguyen, Hoa, and Sherif A. El-Safty. "Meso-and macroporous Co_3O_4 nanorods for effective VOC gas sensors." The Journal of Physical Chemistry C 115, no. 17 (2011): 8466-8474.

N. Li , X. Lu and S. Zhang , A novel reuse method for waste printed circuit boards as catalyst for wastewater bearing pyridine degradation, Chem. Eng. J., (2014): 257 , 253 -261.

N. J. Pachupate and P. D. Vaidya , Catalytic wet oxidation of quinoline over Ru/C catalyst, J. Environ. Chem. Eng., (2018): 883 -889.

Pinto, Lisete DS, Luisa M. Freitas dos Santos, Bushra Al-Duri, and Regina CD Santos. "Supercritical water oxidation of quinoline in a continuous plug flow reactor—part 1: effect of key operating parameters." Journal of Chemical Technology & Biotechnology: International Research in Process, Environmental & Clean Technology 81, no. 6 (2006): 912-918.

Patil, Dewyani, Pradip Patil, Vijayanand Subramanian, Pattayil A. Joy, and Hari S. Potdar. "Highly sensitive and fast responding CO sensor based on Co_3O_4 nanorods." Talanta81, no. 1-2 (2010): 37-43.

Q. Yuan , L. Chen , M. Xiong , J. He , S.-L. Luo , C.-T. Au and S.-F. Yin , $Cu_2O/BiVO_4$ heterostructures: synthesis and application in simultaneous photocatalytic oxidation of organic dyes and reduction of Cr(vi) under visible light, Chem. Eng. J., (2014): 394 -402.

Thomsen, Anne Belinda. "Degradation of quinoline by wet oxidation—kinetic aspects and reaction mechanisms." Water Research 32, no. 1 (1998): 136-146.

Subbaramaiah, V., Vimal Chandra Srivastava, and Indra Deo Mall. "Optimization of reaction parameters and kinetic modeling of catalytic wet peroxidation of picoline by Cu/SBA-15." Industrial & Engineering Chemistry Research 52.26 (2013): 9021-9029.

Subbaramaiah, V., Vimal Chandra Srivastava, and Indra Deo Mall. "Catalytic activity of Cu/SBA-15 for peroxidation of pyridine bearing wastewater at atmospheric condition." AIChE Journal 59.7 (2013): 2577-2586.

Subbaramaiah, V., Vimal Chandra Srivastava, and Indra Deo Mall. "Catalytic wet peroxidation of pyridine bearing wastewater by cerium supported SBA-15." Journal of hazardous materials 248 (2013): 355-363.

Sun, Guang, Honglin Chen, Yanwei Li, Zehua Chen, Saisai Zhang, Guangzhou Ma, Tiekun Jia et al. "Synthesis and improved gas sensing properties of NiO-decorated SnO_2 microflowers assembled with porous nanorods." Sensors and Actuators B: Chemical 233 (2016): 180-192.

Wen, Zhen, Liping Zhu, Weimin Mei, Liang Hu, Yaguang Li, Luwei Sun, Hui Cai, and Zhizhen Ye. "Rhombus-shaped Co_3O_4 nanorod arrays for high-performance gas sensor." Sensors and Actuators B: Chemical 186 (2013): 172-179.

Xiong, Ya, Wangwang Xu, Zongye Zhu, Qingzhong Xue, Wenbo Lu, Degong Ding, and Lei Zhu. "ZIF-derived porous ZnO- Co_3O_4 hollow polyhedrons heterostructure with highly

enhanced ethanol detection performance." Sensors and Actuators B: Chemical 253 (2017): 523-532.

Yin, Kuibo, Jing Ji, Yuting Shen, Yuwei Xiong, Hengchang Bi, Jun Sun, Tao Xu, Zhiyuan Zhu, and Litao Sun. "Magnetic properties of Co_3O_4 nanoparticles on graphene substrate." Journal of Alloys and Compounds 720 (2017): 345-351.

Zhou, J., Q-H. Xia, S-C. Shen, S. Kawi, and K. Hidajat. "Catalytic oxidation of pyridine on the supported copper catalysts in the presence of excess oxygen." Journal of Catalysis 225, no. 1 (2004): 128-137.

Zrnčević, Stanka, and Zoran Gomzi. "CWPO: An environmental solution for pollutant removal from wastewater." Industrial & engineering chemistry research 44, no. 16 (2005): 6110-6114.